Available online at www.sciencedirect.com
ScienceDirect
Journal of Catalysis 251 (2007) 21–27
JOURNAL OF CATALYSIS
www.elsevier.com/locate/jcat

Alkaline-mediated mesoporous mordenite zeolites for acid-catalyzed conversions ☆

Johan C. Groen [a,*], Tsuneji Sano [b], Jacob A. Moulijn [a], Javier Pérez-Ramírez [c,d]

[a] *DelftChemTech, Delft University of Technology, Julianalaan 136, 2628 BL Delft, The Netherlands*
[b] *Department of Applied Chemistry, Graduate School of Engineering, Hiroshima University, Higashi-Hiroshima 739-8527, Japan*
[c] *Institute of Chemical Research of Catalonia (ICIQ), Avinguda Països Catalans 16, 43007 Tarragona, Spain*
[d] *Catalan Institution for Research and Advanced Studies (ICREA), Passeig Lluís Companys 23, 08010 Barcelona, Spain*

Received 7 June 2007; revised 11 July 2007; accepted 13 July 2007

Available online 24 August 2007

Abstract

The preparation of mesoporous mordenite zeolite and its subsequent application in the liquid-phase alkylation of benzene with ethylene is discussed. Mesoporous mordenite was obtained by controlled silicon extraction on alkaline treatment of successfully synthesized high-silica mordenite zeolites with molar Si/Al ratios in the range of 20–30. Besides substantial mesoporosity development, the combined microporous and mesoporous zeolites show preserved Brønsted acidic properties, which are highly attractive when acid-catalyzed reactions are targeted. Catalytic testing of the mesoporous mordenite found superior performance in benzene alkylation due to the unique interplay between improved physical transport in the shortened micropores and the preserved high density of acid sites.

Keywords: Mesoporous mordenite; Zeolites; Porosity; Desilication; Alkylation; Catalysis

1. Introduction

Well-established large-volume hydrocarbon conversions currently used in industry include processes such as catalytic cracking, isomerization, and alkylation [1,2]. In many of these reactions, the traditional liquid acids are progressively substituted with zeolite-based processes [3]. Application of these solid-acid catalysts offers several key advantages. Zeolites are environmentally harmless, noncorrosive, and show ease of separation from the reaction mixture compared with homogeneous catalysts. Moreover, the shape-selective properties of zeolites related to the presence of an ordered microporous network can restrict the formation of undesired products by control of reactant or product diffusion as well as the volume available for transition states. But the purely microporous nature of zeolites frequently poses transport limitations, particularly when bulky molecules are involved. This is typically the case in applications in the petroleum, petrochemical, and fine chemical industries. The restricted mass transfer properties frequently result in lower activities and decreased catalyst lifetime due to deactivation [4].

Mordenite, a member of the large-pore zeolite family, consists of 12-membered ring (MR) pore channels of 0.67 × 0.70 nm interconnected by 8-MR pores of 0.34 × 0.48 nm [5]. Because the 8-MR channels are too small for most molecules to enter, mordenite is generally considered a one-dimensional pore system, inducing single-file diffusion [6]. Despite this feature, mordenite is widely practiced in industry, particularly for alkylation [7] and (hydro)isomerization [8] reactions. To improve physical transport in the one-dimensional channels, mordenite zeolites are typically subjected to dealumination posttreatments [1,7,9,10]. Although dealumination indeed has proven to generate additional mesoporosity [11], this approach directly affects the acidic properties of the zeolite structure, due to the extraction of aluminum from the zeolite framework. The facilitated transport acquired by the introduction of mesoporosity is partially cancelled out by the reduced density of acid

☆ The research in this paper is documented in European patent application EP07109134.2.

* Corresponding author. Fax: +31 15 278 44 52.
E-mail address: J.C.Groen@tudelft.nl (J.C. Groen).

0021-9517/$ – see front matter
doi:10.1016/j.jcat.2007.07.020

sites. This has been confirmed recently by Boveri et al. [12], who investigated the impact of steaming and acid leaching on the physicochemical and catalytic properties of a commercial mordenite catalyst. Their results showed a negligible improved yield of linear alkylbenzene over the variously treated catalysts, despite the development of considerable mesoporosity, which is attributed to a distinct deterioration of the acidic properties. With respect to the acidity required in many zeolite-catalyzed reactions, introduction of mesoporosity while mostly preserving the intrinsic acidic properties would make headway, especially in those structures that are generally modified by dealumination procedures (USY, mordenite, ZSM-5). Specifically, the one-dimensional pore channel system of mordenite will greatly benefit from the introduction of accessible intracrystalline mesoporosity.

In this contribution, we introduce desilicated mordenite zeolite with combined microporous and mesoporosity and unimpaired acidic properties. We prepared the hierarchically structured mordenite through a controlled silicon extraction postsynthesis modification, and used liquid-phase alkylation of benzene with ethylene as a model reaction of industrial relevance to quantitatively demonstrate the benefits of the newly created mesopores and preserved acidity.

2. Experimental

2.1. Materials

High-silica mordenite samples were prepared by direct hydrothermal synthesis with and without seed crystals as described elsewhere [13]. The seed crystals were prepared by mixing NH_4NO_3 (Wako Pure Chemical, 99%) with an aqueous solution of $Al(NO_3)_3{\cdot}9H_2O$ (Wako Pure Chemical, 98%) and NaOH (Merck-Schuchardt, 99%). Subsequently, precipitated hydrated silica (Nipsil, Nippon Silica Ind., 88% SiO_2) and tetraethylammonium hydroxide (Aldrich, 35 wt%) were added to the mixture and homogenized in a mortar. The chemical composition of the starting synthesis gel was $Si/Al = 15$, $NaOH/Al = 3$, $TEAOH/SiO_2 = 0.23$. The obtained gel was transferred to a Teflon-lined stainless steel autoclave and kept at 443 K for 3 days under static conditions. The solid product obtained was filtered, washed with deionized water, and dried at 393 K. The resulting mordenite crystals were then added (4 wt% based on total amount of SiO_2 in the synthesis gel) to the synthesis mixture of high-silica mordenite with molar composition $Si/Al = 30$, $NH_4NO_3/SiO_2 = 0.096$, and $NaOH/Al = 7$. After crystallization at 343 K for 3 days, the final high-silica mordenite sample was obtained (sample code MOR30). Sample MOR20 was synthesized following a similar protocol as for MOR30, but without seeding and with the following molar composition of the synthesis gel: $NH_4NO_3/SiO_2 = 0.046$, $Si/Al = 20$, and $NaOH/Al = 4$. The resulting solids were filtered, washed with demineralized water, dried at 393 K, and finally calcined in static air at 823 K (heating rate 3 K min^{-1}) for 5 h. A commercial mordenite catalyst (CBV20A) was obtained from Zeolyst. Before further investigations, all samples were brought into the ammonium form by three successive ion exchanges in 0.1 M NH_4NO_3, followed by calcination in static air at 823 K for 5 h.

2.2. Alkaline posttreatment

Alkaline treatment of the calcined zeolites was performed in 0.2 M NaOH at 338 K for 30 min, identical to the procedure previously established over ZSM-5 zeolites [14]. After filtration and washing, the zeolites were dried at 373 K and calcined in static air at 823 K. The alkaline-treated samples were converted into the H form by three successive exchanges in 0.1 M NH_4NO_3 solution calcination, followed by in static air at 823 K for 5 h.

2.3. Characterization

Chemical composition of the samples was determined by ICP-OES in a Perkin-Elmer Optima 4300DV. N_2 adsorption at 77 K was carried out in a Quantachrome Autosorb-6B apparatus. Samples were previously evacuated at 623 K for 16 h. The BET surface area was derived from the adsorption isotherm in the adapted relative pressure range of $p/p_0 = 0.01$–0.1. The micropore volume (V_{micro}) and the macro- and mesopore surface area (S_{meso}) were determined with the t-plot method according to Lippens and de Boer. The mesopore size distribution was calculated from the adsorption branch of the isotherm using the Barret–Joyner–Hallenda pore size model. High-resolution, low-pressure argon adsorption measurements were performed after in situ vacuum pretreatment at 623 K for 16 h on a Micromeritics ASAP 2010 to assess the microporous properties. The Saito–Foley pore size model was used to calculate the micropore size distribution. Scanning electron microscopy investigations were carried out at 5 kV in a JEOL JSM-6700F microscope, with the samples coated with palladium to create contrast. Fourier transform infrared (FTIR) spectra were recorded in He at 473 K on a Nicolet Magna 860 Fourier transform spectrometer using a Spectratech diffuse reflectance (DRIFT) accessory, equipped with a high-temperature cell. The sample was pretreated at 723 K in a flow of He to remove any contaminants. Temperature-programmed desorption of ammonia (NH_3-TPD) was carried out in a Micromeritics TPR/TPD 2900 equipped with a thermal conductivity detector (TCD). The sample (30 mg) was pretreated at 873 K in He for 1 h, after which pure NH_3 (25 cm^3 min^{-1}) was adsorbed at 473 K for 10 min. Then a flow of He (25 cm^3 min^{-1}) was passed through the reactor for 25 min to remove weakly adsorbed NH_3 from the zeolite. This procedure was repeated three times. Desorption of NH_3 was monitored in the temperature range of 473–873 K using a heating rate of 10 K min^{-1}.

2.4. Catalytic testing

The activity of the various zeolites was tested in the liquid-phase alkylation of benzene (Aldrich, >99%) with ethylene (Hoekloos, >99.9%) in a 500 cm^3 commercial titanium batch autoclave (Premex). First, 200 cm^3 of benzene was introduced into the reactor with approximately 0.5 g of powdered catalyst

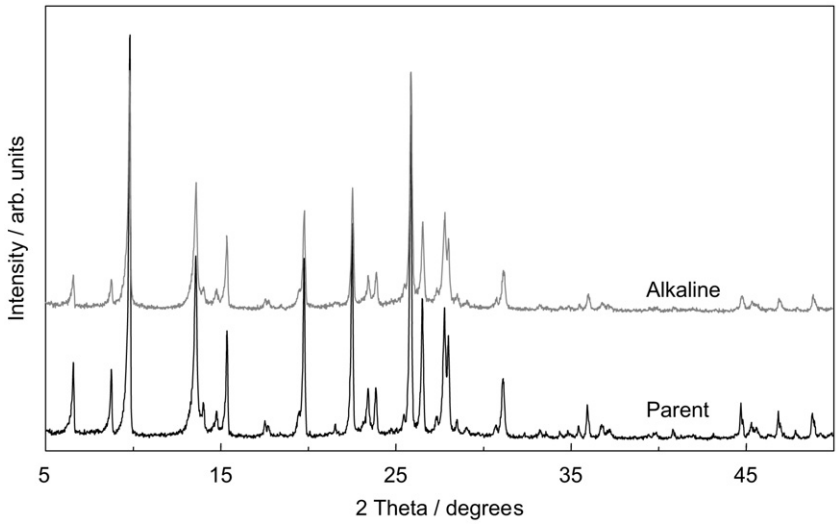

Fig. 1. The XRD patterns of parent and alkaline-treated MOR30 confirm the presence of mordenite as the only crystalline phase and the preserved crystallinity upon alkaline treatment.

Table 1
Textural properties and chemical composition of the parent and alkaline-treated (mesoporous) mordenite samples

Sample	Molar (Si/Al)[a]	V_{micro}[b] ($cm^3\ g^{-1}$)	S_{meso}[b] ($m^2\ g^{-1}$)	NH_3 uptake[c] ($mmol\ g^{-1}$)
MOR20	21	0.21	8	0.80
MOR30	27	0.21	5	0.48
MOR20 alkaline	17	0.19	90	0.78
MOR30 alkaline	19	0.19	115	0.51
MOR10	10	0.20	35	1.18
MOR10 alkaline	10	0.19	40	n.m.

[a] ICP-OES.
[b] *t*-plot method.
[c] NH_3-TPD.

that was previously pretreated at 573 K in He for 12 h to remove moisture. After purging with N_2, the reactor was heated to 438 K under vigorous mechanical stirring (1000 rpm). Subsequently, ethylene was introduced in the reactor until the molar benzene:ethylene ratio was 4:1 and a total pressure of 23 bar was obtained. During the reaction, liquid aliquots (0.2 cm^3) were extracted from the reactor; these were analyzed offline with a Chrompack CP9001 gas chromatograph equipped with a CPSil-8B column and a flame ionization detector.

3. Results and discussion

3.1. Catalyst characterization

Controlled-framework silicon extraction, referred to as desilication [14], was applied to successfully prepare high-quality mesoporous mordenite. The chemical composition and textural characteristics of the parent high-silica mordenite zeolites are summarized in Table 1. It can be concluded that the molar Si/Al ratio of the synthesized samples is 20–30, within the previously identified optimal range for desilication of MFI zeolites [14]. MOR10, a commercial mordenite obtained from Zeolyst (commercial sample code CBV20), was used as a reference catalyst.

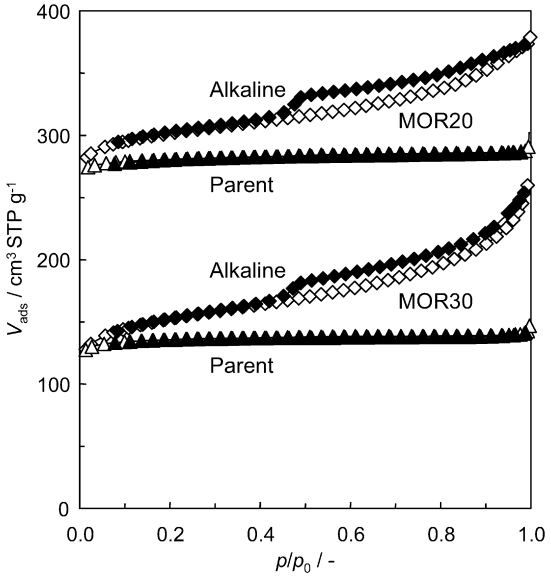

Fig. 2. N_2 adsorption (open symbols) and desorption (solid symbols) isotherms at 77 K of the parent (△, ▲) and alkaline-treated (◇, ◆) zeolites. For sake of clarity, the isotherms of MOR20 have been shifted 150 cm^3 STP g^{-1}.

XRD measurements confirmed the existence of a highly crystalline mordenite displaying sharp reflection lines at the characteristic 2-theta positions (Fig. 1) [15]. The plateau in the N_2 adsorption isotherms of the synthesized materials at higher relative pressures indicates the absence of a major external surface area contribution, whereas the sharp rise in uptake at lower pressure confirms the predominant microporous character of the samples (Fig. 2). The derived micropore volumes of all parent samples in Table 1 are characteristic of the mordenite framework [5]. SEM investigations revealed that the parent samples consisted of aggregated plate-like sheets forming ellipsoidal particles with dimensions of ca. $4 \times 2 \times 2$ μm in MOR30 (Fig. 3), whereas the particles in MOR20 exhibited somewhat larger dimensions of $12 \times 8 \times 5$ μm [13]. In both cases, the crystal size was uniform and displayed no amorphous matter at the

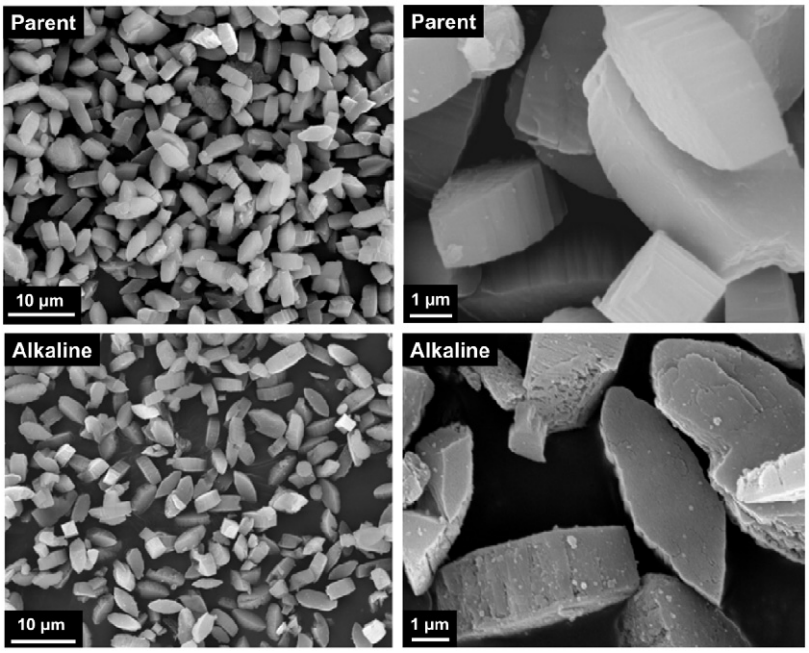

Fig. 3. Low and medium-magnification SEM micrographs of parent (top) and alkaline-treated (bottom) MOR30.

external surface. The relatively large crystal size and the absence of major surface roughness of the parent zeolites account for the observed low mesopore surface areas in Table 1, compared with 35 $m^2\,g^{-1}$ in the commercial MOR10 sample with smaller crystals observed by SEM (ca. 200 nm).

On alkaline treatment of the high-silica zeolites in 0.2 M NaOH at 338 K, i.e. the typical desilication conditions previously applied for ZSM-5 zeolites [14], a distinct hysteresis loop appeared in the N_2 adsorption isotherms of the alkaline-treated samples (Fig. 2). The mesopore surface area increased spectacularly from $<10\ m^2\,g^{-1}$ in the parent samples to 115 and 95 $m^2\,g^{-1}$ in the desilicated materials (Table 1). Interestingly, the micropore volume decreased by only ca. 10%, from 0.21 $cm^3\,g^{-1}$ in the parent samples to 0.19 $cm^3\,g^{-1}$ in the post-treated zeolites. This indicates that besides the high degree of mesoporosity, the alkaline treatment mostly preserved the microporosity in the mordenite crystals. In contrast, alkaline treatment of the commercial MOR10 sample resulted in hardly any new mesopore formation, as could be derived from the overlapping isotherms and the negligible increase in mesopore surface area from 35 to 40 $m^2\,g^{-1}$ (Table 1). This is attributed to the crucial role of framework aluminum in the desilication process previously reported for MFI-type zeolites, in which relatively high concentrations of framework Al was proven to greatly suppress silicon extraction and connected mesoporosity development [14]. Careful selection of the parent zeolites is thus essential to achieve controlled mesoporosity development on alkaline treatment.

High-resolution low-pressure argon adsorption unequivocally demonstrates that the micropore size had not been altered. The adsorption isotherms in Fig. 4 exhibit an analogous behavior at low relative pressures where micropore filling occurs, suggesting that the micropores still exhibited similar adsorption properties and micropore size. The enhanced uptake of

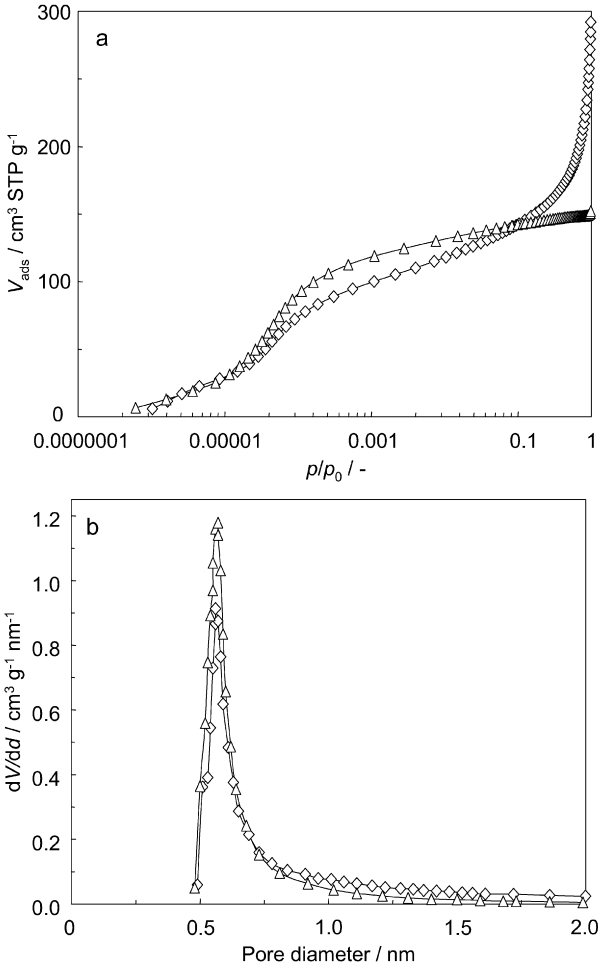

Fig. 4. (a) Argon adsorption isotherms at 87 K and (b) the corresponding Saito-Foley micropore size distribution of parent (△) and alkaline-treated (◇) MOR30.

the alkaline-treated sample at higher relative pressure is associated with the newly created mesoporosity, similar to the results obtained by nitrogen adsorption. The Saito–Foley micropore size distribution further confirms the identical micropore size in the parent and alkaline-treated MOR30 sample and the somewhat lower micropore volume in the latter zeolite. SEM reveals that the mordenite crystals retained their original particle size, emphasizing the intracrystalline nature of the newly created mesoporosity (Fig. 3, bottom). The 12-MR one-dimensional mordenite channels present in the needle-like elongated crystals will be effectively shortened by the successfully incorporated mesoporosity. The more efficient use of the particle volume on introduction of intracrystalline mesopores will be even greater if the parent material suffers from a low actually accessible pore length, due to the presence of, for example, intrapore nonframework species and lattice defects [16,17]. The latter impact can be quite dramatic, provoking an accessible micropore volume down to only 30% of the expected pore length, as was recently revealed by a spatially resolved SEM-EDX study over coked mordenite crystals [16]. Accordingly, shortening the micropore diffusion length by intracrystalline mesoporosity development will open up regions in the micropores in which access originally was restricted. The preserved structural integrity of the mordenite crystals was further substantiated by XRD investigations. The alkaline-treated sample still presented the characteristic fingerprint, but had a significantly lower intensity, obviously as a result of the introduced mesoporosity, leading to an estimated decrease in crystallinity of ca. 10% (Fig. 1).

FTIR analysis and NH_3-TPD measurements confirmed the preserved surface acidity of the alkaline-treated zeolites. This is an essential aspect to ensure an optimal benefit from the improved transport properties in the mesoporous zeolites, particularly when acid-catalyzed reactions are targeted. The FTIR spectrum of the alkaline-treated mordenite maintained the characteristic contribution at 3610 cm^{-1}, the absorption band typically assigned to the Si–OH–Al stretching vibration associated with Brønsted acid sites (Fig. 5) [18]. The absorption at 3740 cm^{-1}, representing isolated silanol groups [19], showed a higher intensity in the alkaline-treated sample, due to the enhanced "external" surface area by the newly created mesopores. In agreement with this finding, the desorption profile of ammonia over MOR30 hardly changed on alkaline treatment and remained centered at around 773 K (Fig. 5). The alkaline-treated sample showed a slightly enhanced contribution at low temperature, giving rise to a moderately increased total uptake from 0.48 mmol g^{-1} in the parent sample to 0.51 mmol g^{-1} in the alkaline-treated zeolite (Table 1). These results indicate that the acidic properties were not significantly altered by the alkaline treatment. In the MOR20 samples, a minimal decrease in total acidity can also be concluded from Table 1. The significant role of framework aluminum for intracrystalline mesopore formation in the desilication process, as previously established over MFI zeolites [14,20], thus appears to be applicable to other zeolite structures, such as mordenite (in the present work) and ZSM-12 [21]. This suggests that the desilication treatment can be universally applied over different zeolite families, provided

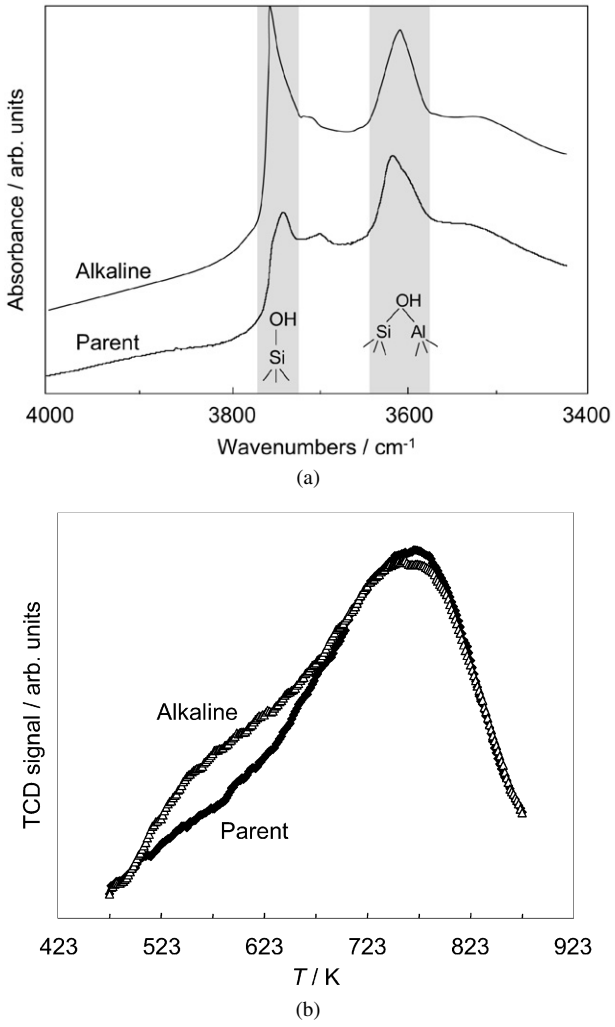

Fig. 5. FTIR spectra in the OH stretching region (a) and NH_3-TPD profiles (b) of parent and alkaline-treated MOR30.

that the Si/Al ratio dependency is adequately taken into account. Moreover, recent work associated with delamination of the lamellar MCM-22 zeolite structure to enhance accessibility, resulting in the ITQ-2 zeolite family as developed by Corma et al. [22], also found a clear dependence of the extraporosity development on the framework aluminum concentration [23]. A low aluminum concentration favors the degree of delamination. This correlation likely can be attributed to the swelling step in the delamination procedure, which is executed at high pH and leads to distinct dissolution of silicon from the zeolite framework, thereby opening the zeolite structure.

3.2. Alkylation performance

Liquid-phase benzene alkylation experiments over the parent and alkaline-treated zeolites were conducted to demonstrate the beneficial role of the mesoporosity on the catalyst performance in the synthesis of ethylbenzene (EB). Application of the reference catalyst MOR10 showed a relatively low productivity of ethylbenzene, corresponding to a final yield of ca. 2% EB with respect to ethylene, mostly related to severe deactivation of the catalyst (Fig. 6). This deactivation is generally

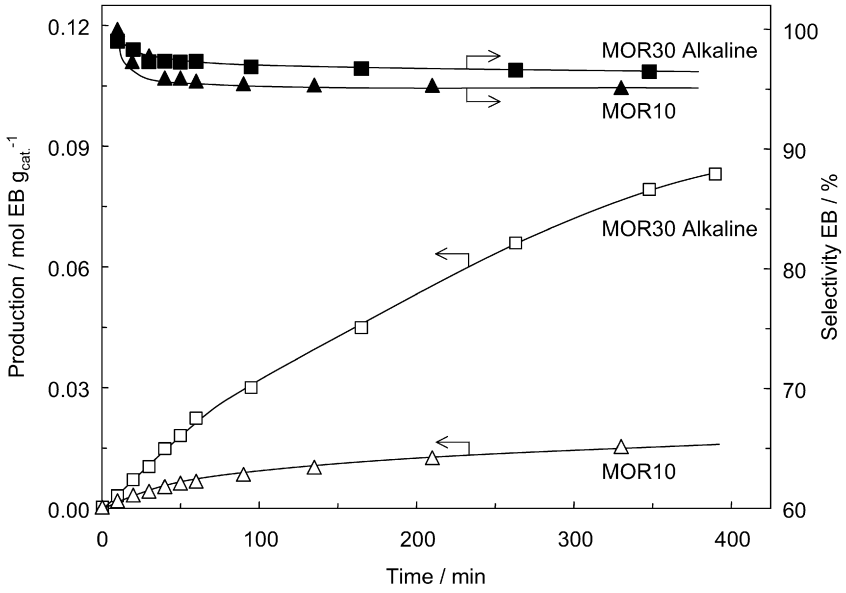

Fig. 6. Ethylbenzene (EB) production (open symbols) and selectivity (solid symbols) over alkaline-treated MOR30 (□, ■) and the reference commercial MOR10 catalyst (△, ▲). The reported selectivity accounts for the primary alkylation products ethylbenzene, diethylbenzene, triethylbenzene, and butylbenzene.

reported to be caused by olefin oligomerization [24], finally leading to coking, which becomes more detrimental when the physical transport of benzene is poor due to, for example, narrow pores or longer micropore diffusion path lengths. Interestingly, the alkaline-treated mesoporous catalyst showed a higher initial activity despite its larger crystal size and lower acidity (Table 1). In addition, the mesoporous mordenite clearly suffered less from deactivation and exhibited an impressive 5- to 6-fold greater EB production.

Importantly, the selectivity toward EB of >96% achieved over the alkaline-treated zeolite was somewhat higher than that observed over the MOR10 catalyst (ca. 95%), even at substantially higher conversion levels. The suppressed deactivation and enhanced selectivity can be attributed to the improved physical transport of reactants and products in the shortened micropores of the alkaline-treated catalyst, similar to what has been reported for mesoporous ZSM-5 crystals obtained by desilication [25]. On one hand, the intracrystalline mesopores facilitate access of benzene to the intrapore active sites, thus leading to more efficient use of the catalyst volume and less ethylene oligomerization. On the other hand, the shortened diffusion path length decreases the average residence time of reacted molecules in the micropores, thereby suppressing successive alkylation steps of ethylbenzene to, for example, diethylbenzene and triethylbenzene. The greater extent of deactivation of the purely microporous catalyst has been confirmed by thermogravimetric and gas adsorption experiments of the spent catalysts. TGA revealed a 2-fold greater amount of coke in the purely microporous commercial catalyst than in the mesoporous mordenite. In addition, N_2 adsorption showed that the former sample had a 7-fold lower micropore volume after reaction, compared with only a 2.5-fold lower volume in the alkaline-treated catalyst. Moreover, complete preservation of the mesoporosity can be concluded in the latter.

3.3. Desilication vs dealumination

To the best of our knowledge, this is the first report of mordenite zeolites with intracrystalline mesoporosity and preserved acidic properties. In particular, the one-dimensional pore structure of mordenite greatly benefits from the introduced mesoporosity compared with two- or three-dimensionally structured zeolites. Previously reported data [26] demonstrated that mesopore surface area improvements obtained by dealumination of mordenite are typically ca. 40–60 $m^2\,g^{-1}$, substantially lower than those acquired in our desilicated mordenite samples. Moreover, a combination of steam treatment and acid leaching often is required to achieve significant mesoporosity development, being highly detrimental to the Al concentration in the resulting materials, leading to molar Si/Al ratios as high as 150. In addition, dealumination treatments have frequently shown to result in encapsulated mesoporosity [27,28], which has been proven to speed up mass transport to a moderate extent [29]. Besides the preserved acidic properties, the opportunity to gain relatively high mesopore surface areas in the desilicated mordenite compared with its dealuminated counterpart makes desilication a superior methodology for preparing mesoporous zeolitic catalysts. Recently reported data on linear alkylbenzene synthesis over variously dealuminated mordenite catalysts, derived from the same reference catalyst MOR10 used in this study, demonstrate that the overall yield of desired product per weight of catalyst is not significantly enhanced by dealumination [12]. The beneficial effect of the moderate mesoporosity development by dealumination is often exceeded by a loss in acidity, resulting in poorer catalytic activity.

Finally, it was recently reported that the crystal size of the high-silica mordenite samples can be tailored by quenching in the course of the crystallization process, still providing a highly crystalline mordenite sample [30]. Application of the alkaline treatment to these submicrometer-sized small crystals

with a molar Si/Al ratio of 20 also substantially enhances the mesopore surface area with 110 $m^2\,g^{-1}$, similar to the large-crystal samples discussed in this contribution. It can be envisaged that a similar degree of mesoporosity development in these submicrometer-sized crystals can offer an even better use of the overall zeolite volume in catalysis and thus a higher catalyst effectiveness coupled to an enhanced stability. This again confirms the vital role of the Si/Al ratio on the mesoporosity development obtained on alkaline treatment.

4. Conclusion

We have shown that desilication of high-silica mordenite in alkaline medium generates substantial intracrystalline mesoporosity while maintaining the microporous and, most importantly, acidic characteristics. Besides the preservation of the intrinsic zeolitic properties, the mesopore surface area achieved in the mesoporous mordenite is superior to that obtained by traditional dealumination posttreatment. Moreover, the successfully prepared mesoporous mordenite strongly suggests the universality of the desilication treatment of zeolites in alkaline medium. The newly obtained mesoporous mordenite leads to improved catalytic performance in the liquid-phase alkylation of benzene with ethylene. Formation of coke by ethylene oligomerization is largely suppressed, and higher productivity and selectivity of ethylbenzene is achieved. The improved catalytic performance is attributed to an enhanced physical transport of molecules in the effectively shortened one-dimensional micropores coupled to preserved acidity.

Acknowledgment

Financial support from Delft University of Technology and the Spanish MEC (Consolider-Ingenio 2010, grant CSD2006-003) is acknowledged

References

[1] K. Tanabe, W.F. Hölderich, Appl. Catal. A 181 (1999) 399.
[2] C. Perego, P. Ingallina, Green Chem. 6 (2004) 274.
[3] F. Rase, Handbook of Commercial Catalysts, CRC Press, Boca Raton, 2000.
[4] M. Guisnet, P. Magnoux, Appl. Catal. 54 (1989) 541.
[5] Ch. Baerlocher, W.M. Meier, D.H. Olson, Atlas of Zeolite Framework Types, fifth ed., Elsevier, Amsterdam, 2001.
[6] G.D. Lei, B.T. Carvill, W.M.H. Sachtler, Appl. Catal. A 42 (1996) 347.
[7] (a) G.S.J. Lee, J.M. Garces, G.R. Meima, M.J.M. van der Aalst, WO/1993/000317 (1993);
(b) W.J. Roth, D.N. Mazzone, B.J. Ratigan, WO/2000/066520 (2000);
(c) J.F. Knifton, P.R. Anantaneni, P.E. Dai, WO/1997/029063 (1997);
(d) P.R. Anantaneni, WO/2000/023404 (2000);
(e) K. Taniguchi, M. Tanaka, K. Takahata, N. Sakamoto, T. Takai, Y. Kurano, M. Ishibashi, WO/1988/003523 (1988).
[8] (a) J.R. Clark, R.J. Wittenbrink, D.F. Ryan, A.E. Schweizer, WO/2000/014184 (2000);
(b) J. Basset, A. Choplin, F. Raatz, A. Theolier, C. Travers, WO/1990/009845 (1990).
[9] S. van Donk, A.H. Janssen, J.H. Bitter, K.P. de Jong, Catal. Rev. Sci. Eng. 45 (2003) 297.
[10] G.S. Lee, J.J. Maj, S.C. Rocke, J.M. Garcés, Catal. Lett. 2 (1989) 243.
[11] A.J. Koster, U. Ziese, A.J. Verkleij, A.H. Janssen, K.P. de Jong, J. Phys. Chem. B 104 (2000) 9368.
[12] M. Boveri, C. Márquez-Álvarez, M. Ángel Laborde, E. Sastre, Catal. Today 114 (2006) 217.
[13] (a) B. Lu, T. Tsuda, Y. Oumi, K. Itabashi, T. Sano, Microporous Mesoporous Mater. 76 (2004) 1;
(b) B. Lu, Y. Oumi, K. Itabashi, T. Sano, Microporous Mesoporous Mater. 81 (2005) 365.
[14] J.C. Groen, L.A.A. Peffer, J.A. Moulijn, J. Pérez-Ramírez, Chem. Eur. J. 11 (2005) 4983.
[15] M.M.J. Treacy, J.B. Higgins, Collection of Simulated XRD Powder Patterns for Zeolites, fourth ed., Elsevier, Amsterdam, 2001.
[16] S. van Donk, J.H. Bitter, A. Verberckmoes, M. Versluijs-Helder, A. Broersma, K.P. de Jong, Angew. Chem. Int. Ed. 44 (2005) 1360.
[17] D. Lozano-Castello, W. Zhu, A. Linares-Solano, F. Kapteijn, J.A. Moulijn, Microporous Mesoporous Mater. 92 (2006) 145.
[18] A. Zecchina, S. Bordiga, G. Spoto, D. Scarano, G. Petrini, G. Leofanti, M.J. Padovan, Chem. Soc. Faraday Trans. 88 (1992) 2959.
[19] A. Zecchina, S. Bordiga, G. Spoto, L. Marchese, G. Petrini, G. Leofanti, M.J. Padovan, Phys. Chem. 96 (1992) 4991.
[20] J.C. Groen, J.C. Jansen, J.A. Moulijn, J. Pérez-Ramírez, J. Phys. Chem. B 108 (2004) 13062.
[21] X. Wei, P. Smirniotis, Microporous Mesoporous Mater. 97 (2006) 97.
[22] A. Corma, V. Fornés, S.B.C. Pergher, Th.L. Maesen, J.G. Buglass, Nature 396 (1998) 353.
[23] P. Frontera, F. Testa, R. Aiello, S. Candamano, J.B. Nagy, Microporous Mesoporous Mater. (2007), doi:10.1016/j.micromeso.2007.02.031.
[24] (a) G. Bellussi, G. Pazzuconi, C. Perego, G. Girotti, G. Terzoni, J. Catal. 157 (1995) 227;
(b) A. Corma, V. Martínez-Soria, E. Schnoeveld, J. Catal. 192 (2000) 163.
[25] J.C. Groen, W. Zhu, S. Brouwer, S.J. Huynink, F. Kapteijn, J.A. Moulijn, J. Pérez-Ramírez, J. Am. Chem. Soc. 129 (2007) 355.
[26] (a) S. van Donk, A. Broersma, O.L.J. Gijzeman, J.A. van Bokhoven, J.H. Bitter, K.P. de Jong, J. Catal. 204 (2001) 272;
(b) M.A. Hernández, V. Petranovskii, M. Avalos, R. Portillo, F. Rojas, V.H. Lara, Sep. Sci. Technol. 41 (2006) 190;
(c) J. Wang, J.-N. Park, Y.-K. Park, S.Y. Han, J.-O. Baeg, C.W. Lee, Catal. Today 97 (2004) 283;
(d) M. Haouas, S. Bernasconi, A. Kogelbauer, R. Prins, Phys. Chem. Chem. Phys. 3 (2001) 5067.
[27] D. Vergani, R. Prins, H.W. Kouwenhoven, Appl. Catal. A 163 (1997) 71.
[28] A.H. Janssen, A.J. Koster, K.P. de Jong, Angew. Chem. Int. Ed. 40 (2001) 1102.
[29] P. Kortunov, S. Vasenkov, J. Kärger, R. Valiullin, P. Gottschalk, M. Fé Elía, M. Perez, M. Stöcker, B. Drescher, L.D. McKeever, C. Berger, R. Gläser, J. Weitkamp, J. Am. Chem. Soc. 127 (2005) 13055.
[30] B. Lu, Y. Yakushi, Y. Oumi, K. Itabashi, T. Sano, Microporous Mesoporous Mater. 95 (2006) 141.